Vol. 94 (1998) ACTA PHYSICA POLONICA A No. 2

Proc. of the XXVII Intern. School on Physics of Semiconducting Compounds, Jaszowiec 1998

# IV–VI SEMIMAGNETIC SEMICONDUCTORS: RECENT DEVELOPMENTS*

T. STORY

Institute of Physics, Polish Academy of Sciences
Al. Lotników 32/46, 02-668 Warsaw, Poland

Recent developments in the field of semimagnetic IV–VI semiconductors are discussed with the emphasis on magnetic properties of bulk crystals with rare-earth ions (e.g., $Sn_{1-x}Gd_xTe$, $Pb_{1-x}Ce_xSe$, $Pb_{1-x}Eu_xTe$) and new low-dimensional magnetic multilayers (PbTe–EuTe and PbS–EuS). The other issues addressed, concern the new results in transport properties of ferromagnetic $Pb_{1-x-y}Sn_yMn_xTe$, the observation of the Knight shift in electron paramagnetic resonance in PbTe:Mn and SnTe:Mn, and the thermoelectric properties of PbTe–$Pb_{1-x}Eu_xTe$ quantum wells.

PACS numbers: 75.20.Ck, 75.30.Et

## 1. Introduction

IV–VI semimagnetic semiconductors form the well-known group of semiconducting alloys (substitutional solid solutions) in which the presence of magnetic ions and their exchange interaction with carriers in the conduction and in the valence band results in a number of new effects. These, for example, are the carrier concentration induced paramagnet–ferromagnet and ferromagnet–spin glass transitions [1, 2], and large temperature and magnetic field dependent spin splittings of band states [3]. The specific properties of IV–VI matrices make the IV–VI semimagnetic semiconductors a particularly interesting object of research. They show, in particular, semimetallic electric properties and allow for a simple control of carrier concentration by means of doping or isothermal annealing. As opposed to II–VI semimagnetic materials, IV–VI crystals are known to form solid solutions not only with magnetic ions from $3d$ group (like Mn), but also with the elements of $4f$ group (Eu, Gd, Ce, Yb) [3–5] and the elements of $5f$ group (U) [6].

The recent studies in the field of IV–VI semimagnetic semiconductors concerned magnetic, transport, and magnetooptical properties of both bulk crystals and epitaxial structures and resulted in a number of interesting developments which will be presented in this paper. Out of a quite long list of new results,

*This work was partially supported by the Committee for Scientific Research grant No. 2 P03B 109 12.

the following points will be discussed: magnetic properties of bulk IV–VI crystals with rare-earth ions, transport properties of ferromagnetic $Pb_{1-x-y}Sn_yMn_xTe$ and paramagnetic $Pb_{1-x}Eu_xTe$, magnetic properties of new magnetic multilayers EuTe–PbTe and EuS–PbS, the effect of the Knight shift in electron paramagnetic resonance in PbTe:Mn and SnTe:Mn, and the application of PbTe–$Pb_{1-x}Eu_xTe$ multiple quantum wells in new thermoelectric systems.

## 2. Rare-earth ions based IV–VI semimagnetic semiconductors

The IV–VI semimagnetic materials with Eu as well as the low-dimensional structures incorporating these materials are, at the moment, the most actively studied IV–VI semimagnetic materials. The research concerns, in particular, magnetooptical studies of $Pb_{1-x}Eu_xSe$ and $Pb_{1-x}Eu_xTe$ layers and PbTe-$Pb_{1-x}Eu_xTe$ multiple quantum wells [7, 8]. The application of the powerful coherent anti-Stokes Raman scattering (CARS) technique provides very detailed information on the band structure parameters. It is also a valuable source of the information on the $sp-f$ exchange integrals. The transport properties as well as the applications of these materials will be discussed below.

An extensive work concerns the application of the so-called magnetization steps method to the study of the $f-f$ exchange interactions between Eu ions in $Pb_{1-x}Eu_xTe$, $Pb_{1-x}Eu_xSe$ and $Pb_{1-x}Eu_xS$ [9–11]. The interesting experimental result is the discovery of the fact that the magnetic exchange interaction between nearest Eu neighbors is the dominant antiferromagnetic interaction. This is in contrast to EuS and EuTe crystals where this interaction is ferromagnetic, and the interaction between Eu next nearest neighbors provides the strongest antiferromagnetic coupling. Since both diluted materials (like $Pb_{1-x}Eu_xS$) and magnetic semiconductors (like EuS) crystallize in the same NaCl structure with almost equal lattice constants and the same anion sublattice, the physical reason for this qualitative difference seems to be the different electronic structure of these two materials. This point merits a further research.

Apart from the Eu-based IV–VI semimagnetic semiconductors the crystals with Gd such as $Sn_{1-x}Gd_xTe$ [4, 12] and $Pb_{1-x-y}Sn_yGd_xTe$ [13] are also investigated. The research in this field was recently reviewed in Ref. [4]. The IV–VI materials with other rare-earth ions are now available for research. These, in particular, are $Pb_{1-x}Ce_xSe$ [5].

As the new information about the electronic and magnetic properties of IV–VI semimagnetic semiconductors with different rare-earth ions becomes available one might consider the following difference between the "standard" materials with Mn (like $Pb_{1-x}Mn_xTe$) and the new materials with Eu (like $Pb_{1-x}Eu_xTe$). The scheme of the model of the electronic band structure used in the analysis of the magnetic and electronic properties of PbMnTe is presented in Fig. 1. One of the characteristic points is that the density of states (DOS) originating from the electronic states of magnetic $3d^5$ shell of Mn is located about 3.5 eV below the top of the valence band of PbMnTe. Depending on the doping (or annealing) the Fermi level position encountered in PbMnTe is shown by the line labeled $E_F$. It is clear that by changing the Fermi level position (by doping) or by changing the energy gap (by varying Mn content), one does not "disturb" the DOS derived from

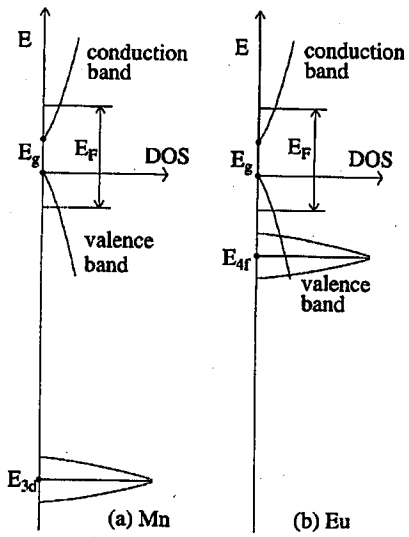


Fig. 1. The scheme of the density of states for $Pb_{1-x}Mn_xTe$ (a) for $Pb_{1-x}Eu_xTe$ (b). The range of Fermi level positions encoutered in these crystals depending on doping or annealing conditions is marked with $E_F$.

Mn $3d^5$ states. Consequently, there is no effect of Mn ions on carrier concentration and their magnetic moments have a well-defined local character. For PbEuTe crystals, one expects a qualitatively similar picture but the center of gravity of DOS derived from the Eu $4f^7$ states is only 1 eV below the top of the valence band [14, 15]. By increasing the band gap (via increasing Eu content) one might expect that, in $p$-type crystals, the Fermi level might appear rather close to the DOS derived from the Eu ions $4f^7$ states. It might result in an important change of both magnetic and electronic properties. This possibility was not yet convincingly demonstrated experimentally.

## 3. Transport properties

Recently, the experimental investigations of magnetic, transport, and thermal properties of ferromagnetic $Pb_{1-x-y}Sn_yMn_xTe$ semiconductors have been performed in the entire Mn composition range available with the quasi-equilibrium bulk crystal growth techniques ($x < 0.15$) [16, 17]. In particular, the systematic study of the transport properties have been carried out. The strong anomalous Hall effect (AHE) was observed in PbSnMnTe crystals with a high Mn content. In early studies performed for the samples with low Mn content, AHE was barely observed requiring an application of a special ac current ac magnetic field technique [18]. In crystals with $x = 0.12$, the AHE gives the dominant contribution to the Hall voltage (see Fig. 2). The AHE is known to arise from asymmetric (skew) scattering mechanisms, when the probabilities of the scattering of carrier to the right or to the left side of the scattering center are different. It requires a spin–orbit interaction to be important either in the scattering potential of the center or in the electronic wave function of the conducting carrier. The experimental analysis of

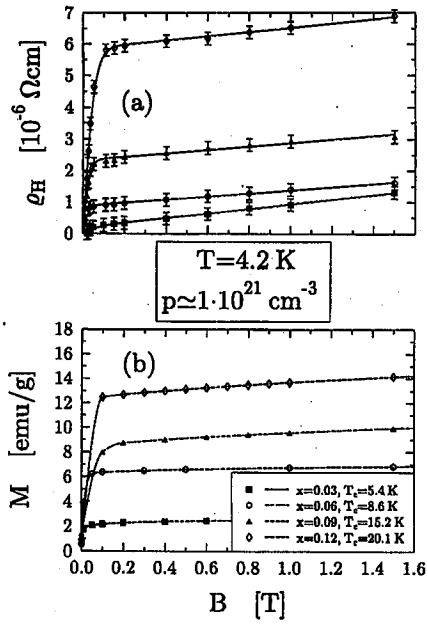


Fig. 2. The magnetic field dependence of the Hall resistivity (a) and the magnetization (b) of ferromagnetic $Pb_{1-x-y}Sn_yMn_xTe$ with $y \approx 0.7$ and Mn composition indicated in the figure.

this effect was performed as a function of the concentration of native defects (metal vacancies) and the concentration of Mn ions. It was shown that the non-magnetic scattering centers (vacancies in metal sublattice) are quite efficient asymmetric scattering centers. It is related to an important role of spin–orbit interactions for the band structure of IV–VI semiconductors.

In the layers of different semimagnetic semiconductor, namely $Pb_{1-x}Eu_xTe$ the metal–insulator transition was discovered [19]. The transition to the, unusual for IV–VI materials, semi-insulating state is driven by a strong alloy scattering. The unusually strong effect of alloy scattering is due to the large scattering potential as given by the large band offset between the conduction bands of PbTe and EuTe.

## 4. Electron paramagnetic resonance Knight shift

The electron paramagnetic resonance (EPR) studies of IV–VI semimagnetic semiconductors have, from the very beginning of the research on these materials, provided important information on, e.g., the charge state of magnetic ions, the $sp-d$ exchange integrals and the role of crystal field effects [20]. One of the effects expected theoretically and long searched experimentally is the Knight shift in EPR. It is the EPR analog of the well-known Knight shift in nuclear magnetic resonance (NMR). Experimentally, it is observed as a shift of the EPR resonance field (the change of the $g$-factor of magnetic ion, $g_M$) with the change of the concentration of carriers: $\Delta g_M = J_{sp-d} g_e \rho(E_F)$, where $J_{sp-d}$ is the carrier–magnetic ion exchange

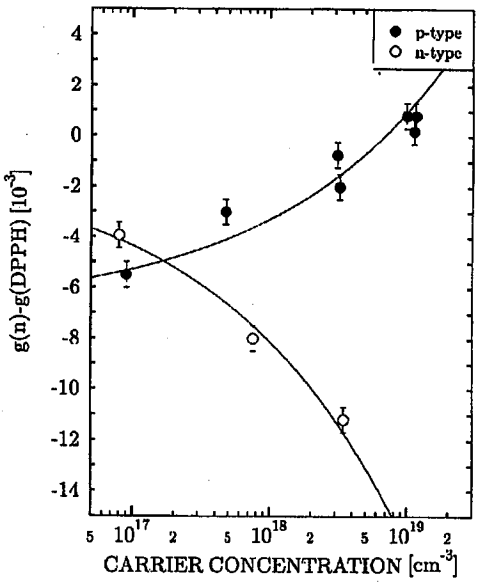


Fig. 3. The carrier concentration dependence of the $Mn^{2+}$ ions EPR $g$-factor in $n$- and $p$-type $Pb_{1-x}Mn_xTe$ with $x = 0.0003 \div 0.001$.

interaction integral, $g_e$ is the $g$-factor of conducting carriers and $\rho(E_F)$ is the density of states at the Fermi level. The physical origin of this effect is the presence of the molecular field due to spin polarization of conducting carriers induced by the $sp-d$ exchange coupling. The first successful direct experimental observation of the Knight shift in EPR was performed in $Pb_{1-x}Mn_xTe$ and $Sn_{1-x}Mn_xTe$ crystals with $x = 0.001$ and $x = 0.0003$ [21]. This result is presented in Fig. 3 for both $n$- and $p$-type PbTe:$Mn^{2+}$. The solid lines are calculated taking into account the effect of nonparabolicity on both conducting carriers $g$-factor and on the density of states. The analysis of these experiments yields both the sign and the magnitude of the exchange integral $J_{sp-d}$. The EPR Knight shift might become a valuable experimental tool to study the local carrier concentration in, e.g., complicated semiconducting structures or in active regions of semiconducting devices.

## 5. Low-dimensional magnetic structures

The magnetic properties of multilayer structures composed of magnetic and nonmagnetic layers are currently one of the most important basic and application fields of research in magnetism. Particularly important are the interlayer exchange interactions, thickness dependence of magnetic anisotropy and magnetic transition temperature and magnetoresistance of such a structure. Although most of the research concerns metallic systems such as Co–Cu, there is a considerable interest in magnetic structures with semiconducting layers. In particular, the use of the well-known magnetic semiconductors seems to be a natural choice for the magnetic structures composed entirely of semiconducting materials with the high standards for the multilayer quality.

The best studied structure is EuTe–PbTe/$BaF_2$ (antiferromagnet–diamagnet) system grown by molecular beam epitaxy [22–25]. The neutron diffraction studies of these structures have demonstrated the presence of the specific satellite magnetic diffraction peaks indicating the existence of the exchange interaction between antiferromagnetic EuTe layers via the diamagnetic PbTe layer. This interlayer coupling was found to be quite long ranged and to persist up to about 50 Å of the separation distance between magnetic layers [22]. The model calculations as well as the quantitative analysis of the neutron diffraction data have been recently performed [25].

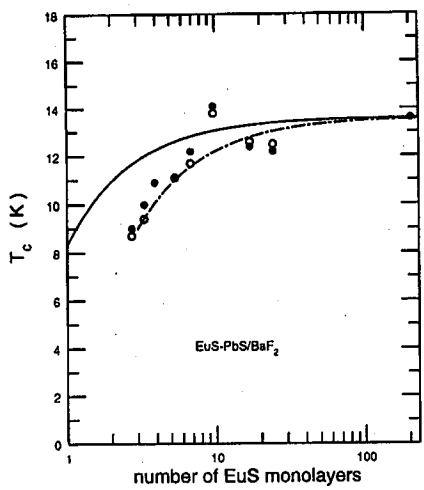


Fig. 4. The thickness dependence of ferromagnetic transition temperature in EuS–PbS/$BaF_2$. The open and full points corresponds to two different methods used for the determination of the Curie temperature.

The other semiconducting magnetic system currently studied is EuS–PbS/$BaF_2$ and EuS–PbS/KCl, where EuS is the well-known ferromagnetic semiconductor and PbS is diamagnetic perfectly lattice matched counterpart layer. The experimental studies of the dependence of ferromagnetic temperature on the thickness of the magnetic layer have shown the decrease in the ferromagnetic Curie temperature for ultrathin layers of EuS. The experimental results for EuS–PbS/$BaF_2$ are presented in Fig. 4 [26]. The effect is described by a simple mean-field approach taking into account the effect of a decreased number of magnetic neighbors for spins located close to the interface with PbS. The experimental results are well reproduced if a 1-monolayer interface mixing is taken into account. The other interesting system which forms the semiconducting ferromagnet– diamagnet multilayer is $Sn_{1-x}Mn_xTe$–SnTe/$BaF_2$. Here semimagnetic SnMnTe is a ferromagnetic layer. The research in this system is at a quite early stage. The recent results obtained for thick MBE grown SnMnTe layers are presented in Ref. [27].

## 6. Applications

IV–VI semiconductors PbTe, PbSe, PbS, SnTe, and their ternary and quaternary alloys are relevant for two fields of applications. First, they are good infrared detectors and lasers, which (owing to the use of mixed crystals like $Pb_{1-y}Sn_yTe$) cover the broad range of infrared part of the spectrum of electromagnetic radiation [28, 29]. Despite rather low financial funding available for the development of the new infrared optoelectronic devices based on IV–VI semiconductors, the impressive progress has been achieved in heterostructure lasers incorporating semimagnetic materials such as $Pb_{1-x}Eu_xTe_{1-y}Se_y$. Mid-infrared lasers with PbTe–PbEuTeSe heterostructure operate (in continuous wave mode) above $T = 200$ K, and, in this range of spectrum, can compete with lasing structures made of III–V low-dimensional systems.

The physical property of PbEuTeSe layers which is explored in these applications is the very efficient band gap and refractive index engineering realized via the composition dependence of the energy gap characterized by the large coefficient $dE_g/dx \approx 5$ eV. The use of semimagnetic materials in new optoelectronic devices is not followed by the use of semimagnetic phenomena. In IV–VI semimagnetic materials with Eu, the $sp-f$ exchange integrals are small [3] and magnetizations encountered are rather low. It leads to the necessity to cool the perspective new semimagnetic devices down to liquid helium temperatures which seriously limits the application field of these devices.

The second field of applications concerns thermoelectric generators and thermoelectric (Peltier) refrigerators. PbTe is one of few semiconducting materials used, e.g., by NASA, for the production of radioactive thermoelectric power gen-

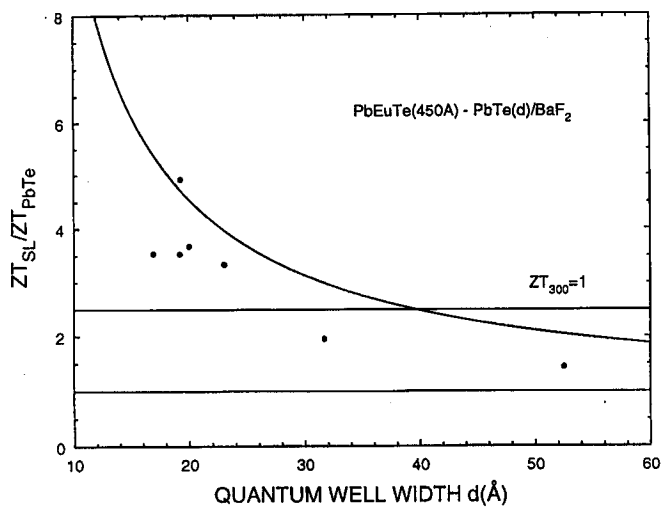


Fig. 5. The well width dependence of the thermoelectric figure of merit $ZT_{SL}$ for PbTe–PbEuTe quantum wells as normalized per the value of this parameter for bulk crystals of PbTe $ZT_{PbTe}$.

erators for satellites [30–33]. The applicational potential of a given thermoelectric material is characterized by the dimensionless figure of merit parameter $ZT$, where $Z = \alpha^2\sigma/\kappa$ and $T$ is temperature [30, 31]. Here, $\alpha$ is the thermoelectric power, $\sigma$ is the electric conductivity and $\kappa$ is the thermal conductivity (both electronic and lattice part). The materials used in thermoelectric coolers are $Bi_2Te_3$–$Bi_2Se_3$–$Sb_2Te_3$ alloys. For the thermoelectric generators, $Si_{1-x}Ge_x$ alloys or doped PbTe crystals are used [30]. Each of these systems has $ZT_{300K} \leq 1$ which makes the overall efficiency of these devices not competitive to other cooling or power generating systems. The recently renewed search for the new materials with $ZT_{300K} > 1$ has resulted in the discovery of the interesting thermoelectric properties of multiple quantum wells, in particular the system PbTe–$Pb_{1-x}Eu_xTe$. It was demonstrated, both theoretically [32] and experimentally [33], that such a multilayer system may show thermoelectric properties superior to bulk crystals (see Fig. 5). The physical origin of this effect stems from the strong modification of the energy dependence of the density of states in two-dimensional systems as compared to three-dimensional ones. The observed increase in the thermoelectric figure of merit might be of big practical importance. It is not clear yet, whether these new physical properties discovered in model quantum structures will result in a new generation of thermoelectric devices [30, 31].

## 7. Summary

In summary, the recent experimental studies of IV–VI semimagnetic semiconductors provided a lot of interesting results important, in particular, for the understanding of magnetic, magnetooptical and transport properties of both bulk crystals and low-dimensional structures. The field of magnetic multilayers composed of EuTe (or EuS) and relevant IV–VI semiconductor has proven to be a valuable alternative for the study of model magnetic multilayers. For applications, the primary point of current interest is the verification of the applicability of the recently studied thermoelectric properties of PbTe–PbEuTe multiple quantum wells into the design of the actual devices.

## References

[1] T. Story, *Acta Phys. Pol. A* **91**, 173 (1997).

[2] W.J.M. de Jonge, T. Story, H.J.M. Swagten, P.J.T. Eggenkamp, *Europhys. Lett.* **17**, 631 (1992).

[3] G. Bauer, H. Pascher, W. Zawadzki, *Semicond. Sci. Technol.* **7**, 703 (1992).

[4] T. Story, *Acta Phys. Pol. A* **92**, 663 (1997).

[5] X. Gratens, S. Charar, M. Averous, S. Isaber, J. Deportes, Z. Gołacki, *Phys. Rev. B* **56**, 8199 (1997).

[6] S. Isaber, C. Fau, S. Charar, M. Averous, Z. Gołacki, *Mater. Sci. Forum* **182-184**, 657 (1995).

[7] S. Yuan, H. Krenn, G. Springholz, Y. Ueta, G. Bauer, *Phys. Rev. B* **55**, 4607 (1997).

[8] F. Geist, W. Herbst, C. Mejia-Garcia, H. Pascher, R. Rupprecht, Y. Ueta, G. Springholz, G. Bauer, M. Tacke, *Phys. Rev. B* **56**, 13042 (1997).

[9] S. Isaber, S.K. Misra, S. Charar, X. Gratens, M. Averous, Z. Gołacki, *Phys. Rev. B* **56**, 13724 (1997).

[10] E. ter Haar, V. Bindilatti, N.F. Oliveira, Jr., G.H. McCabe, Y. Shapira, Z. Gołacki, S. Charar, M. Averous, E.J. McNiff, Jr., *Phys. Rev. B* **56**, 8912 (1997).

[11] V. Bindilatti, E. ter Haar, N.F. Oliveira, Jr., M.T. Liu, Y. Shapira, X. Gratens, S. Charar, S. Isaber, P. Masri, M. Averous, Z. Gołacki, E.J. McNiff, Jr., *Phys. Rev. B* **57**, 7854 (1998).

[12] M. Górska, J.R. Anderson, C. Wolters, A. Łusakowski, T. Story, Z. Gołacki, *Acta Phys. Pol. A* **94**, 347 (1998).

[13] T. Story, M. Arciszewska, P. Łazarczyk, A. Łusakowski, M. Górska, W. Dobrowolski, B. Witkowska, E. Grodzicka, R.R. Gałązka, *Acta Phys. Pol. A* **92**, 997 (1997).

[14] R. Denecke, L. Ley, G. Springholz, G. Bauer, *Phys. Rev. B* **53**, 4534 (1996).

[15] Y. Iida, T. Shimizu, H. Enomoto, H. Ozaki, *Jpn. J. Appl. Phys.* **32**, 4449 (1993).

[16] P. Łazarczyk, T. Story, A. Jędrzejczak, R.R. Gałązka, W. Mac, M. Herbich, A. Stachow-Wójcik, *J. Magn. Magn. Mater.* **176**, 233 (1997).

[17] P. Łazarczyk, T. Story, M. Arciszewska, R.R. Gałązka, *J. Magn. Magn. Mater.* **169**, 151 (1997).

[18] A.M. Sandauer, *Phys. Status Solidi A* **111**, K219 (1989).

[19] Y. Ueta, A. Prinz, G. Grabecki, G. Springholz, G. Brunthaler, T. Dietl, G. Bauer, in: *Proc. 8th Int. Conf. Narrow Gap Semiconductors*, Eds. S.C. Shen, D.Y. Tang, G.Z. Zheng, G. Bauer, World Scientific, Singapore 1998, p. 93.

[20] T. Story, P.J.T. Eggenkamp, C.H.W. Swüste, H.J.M. Swagten, W.J.M. de Jonge, A. Szczerbakow, *Phys. Rev. B* **47**, 227 (1993) and references therein.

[21] T. Story, C.H.W. Swüste, P.J.T. Eggenkamp, H.J.M. Swagten, W.J.M. de Jonge, *Phys. Rev. Lett.* **77**, 2802 (1996).

[22] T.M. Giebultowicz, V. Nunez, G. Sprinholz, G. Bauer, J. Chen, M.S. Dresselhaus, J.K. Furdyna, *J. Magn. Magn. Mater.* **140-144**, 635 (1995).

[23] Z. Wilamowski, G. Springholtz, V. Svrcek, W. Jantsch, *Acta Phys. Pol. A* **92**, 1051 (1997).

[24] L. Bergomi, J.J. Chen, *Phys. Rev. B* **56**, 3281 (1997).

[25] J. Blinowski, P. Kacman, *Acta Phys. Pol. A* **92**, 719 (1997).

[26] A. Stachow-Wójcik, A. Twardowski, T. Story, W. Dobrowolski, E. Grodzicka, A. Sipatov, *Acta Phys. Pol. A* **92**, 985 (1997).

[27] A.J. Nadolny, J. Sadowski, T. Story, W. Dobrowolski, M. Arciszewska, K. Świątek, J. Kachniarz, J. Adamczewska, *Acta Phys. Pol. A* **94** (1998), *Proc. of this Conf. (Part II)*.

[28] Z. Feit, M. McDonald, R.J. Woods, V. Archambault, P. Mak, *Appl. Phys. Lett.* **68**, 738 (1996).

[29] M. Tacke, *Infrared Phys. Tech.* **36**, 447 (1995).

[30] G.D. Mahan, *Solid State Physics*, Vol. 51, Academic Press, New York 1998, p. 81.

[31] G.D. Mahan, B. Sales, J. Sharp, *Phys. Today* **50**, (3), 42 (1997).

[32] L.D. Hicks, M.S. Dresselhaus, *Phys. Rev. B* **47**, 12727 (1993).

[33] L.D. Hicks, T.C. Harman, X. Sun, M.S. Dresselhaus, *Phys. Rev. B* **53**, R10493 (1996).